

## **Supplemental information**

### **Supplemental materials and methods**

#### **HCC cell lines and tissues**

The human HLE, HLF, Hep3B, SNU-368, SNU-398, SNU-739, Huh7, MHCC97H and THLE-2 HCC cell lines were routinely cultured in Dulbecco's DMEM or RPMI-1640 medium enriched with 10% fetal bovine serum (HyClone Laboratories), as well as 100 µg/mL of streptomycin under humid 5% CO<sub>2</sub> conditions at 37°C. Moreover, 247 paired (30 paired for qRT-PCR and Western blotting assays; 217 paired for IHC staining assay) human HCC tumor and peritumor tissue samples as well as 36-unpaired primary and metastatic HCC tissue samples were acquired from the Xijing Hospital of the Fourth Military Medical University in Xi'an, China, as previously described[1]. The Ethical Committee of the Fourth Military Medical University (Xi'an, China) approved this study and written consents were obtained from all participants.

#### **qRT-PCR**

Total RNA from HCC cell lines or tissues were extracted using the Trizol Reagent (Invitrogen, 15596018) and reverse transcribed into cDNA using a PrimeScript RT Reagent kit, as per the manufacturer's protocol. qRT-PCR was performed using a SYBR Green PCR Kit (Takara, 639676). The  $2^{-\Delta\Delta CT}$  approach was used to determine relative expressions of target genes. The housekeeping-gene ( $\beta$ -actin) was the internal standard. The primers used in this assay are shown in **Supplementary Table 2**.

#### **Western blotting**

Total proteins were purified from HCC cell lines or tissues as described previously[2]. Protein concentrations were determined via the BCA assay (Bio-Rad Laboratories). Equivalent protein amounts were resolved on SDS–polyacrylamide gels, electroblotted onto PVDF membranes and incubated overnight at 4 °C in the presence of specific primary antibodies. Relative protein expressions of target genes were determined after incubation at room temperature for 2 h in the presence of appropriate secondary horseradish-peroxidase-labeled antibodies. Visualization was performed via an enhanced chemiluminescence assay. The primary antibodies in this assay and their working concentrations are shown in **Supplementary Table 2**.

#### **H&E and immunohistochemistry staining**

H&E and immunohistochemistry staining were performed as previously described[3]. Immunostains were scored based on positive staining cell proportions and staining intensity[3]. Primary antibodies in this assay and their working concentrations are specified in **Supplementary Table 2**.

#### **Flow cytometry analysis for cell cycle and apoptosis**

For cell cycle analysis, HCC cells with different treatments were fixed in 70% ethanol at 4°C overnight, stained with propidium iodide (BestBio, shanghai, China) at room temperature for 30 min, and assessed by flow cytometry (Beckman, Fullerton, CA). For cell apoptosis analysis, the FITC-Annexin V and PI Apoptosis Kit (F6012, US EverbrightInc) was used. A total of 5 µl ANXA5-FITC and 5 µl PI were introduced into HCC cells and incubated at room temperature for 20 min in the dark. Cells were rinsed thrice using PBS and analyzed by flow cytometry (Beckman,

Fullerton, CA).

### **Wound-healing, cell migration and matrigel invasion assays**

To determine cell migration abilities, a pipette tip was used to scratch the middle of wells when cells in the 6-well plates had achieved a 85% confluence. Imaging of wound-closures was performed using a light Olympus microscope at 0 and 48 h after scratching. Relative migrations of differentially treated HCC cells were determined using the Image J software. For matrigel invasion assessment, transwell chambers coated with the matrigel matrix (BD Science) were used. Briefly,  $1 \times 10^5$  cells were loaded into the upper chamber of each well. After 48 h of incubation in a 5% CO<sub>2</sub> atmosphere at 37°C, cells that had invaded the lower chamber were fixed in 4% formaldehyde for 10 min and stained with 0.1% crystal violet for 10 min at room temperature. The number of invaded cells in each group was determined by light microscopy.

### **Reporter plasmids and site-directed mutagenesis**

Promoter sequences of GPAM were abstracted from the UCSC Genome Browser. Truncated portions of the GPAM promoter amplified by PCR at selected regions were inserted into pGL3-Basic vectors (Promega, Madison, WI). The primer sequences used in this study are indicated in supplementary Table 1. Site-directed mutagenesis was performed using a Q5 Site-Directed Mutagenesis Kit (NEB, E0552S) as instructed by the manufacturer.

### **Immunofluorescence**

For double immunofluorescence staining of BMAL1 and EZH2, HCC cells were

plated in the culture dish and incubated with primary BMAL1 and EZH2 antibodies at 4°C overnight. After rinsing twice in PBS, they were respectively incubated with 488-labelled goat anti-rabbit or 594-labelled goat anti-mouse secondary antibodies. Counterstaining of the nucleus was performed using 4', 6-diamidino-2-phenylindole (DAPI) followed by imaging using an Olympus FV 1000 laser-scanning confocal microscope.

### **ELISA for determination of lipid levels**

The amounts of glycerolipid synthesis products (LPA, PA, DAG, TAG) in HCC cells were measured using the avidin biotin system (ABS) antibody sandwich ELISA method. The LPA, PA, DAG, and TAG kits (human, 96-well) were purchased from mlbio (shanghai). Based on the instructions, intracellular components of HCC cells ( $1 \times 10^6$  cells/ml) were extracted and quantitated by ELISA. Assays were performed as described [4, 5].

### ***In vivo* tumorigenicity and metastatic assays**

To assess the *in vivo* tumor growth,  $1 \times 10^7$  HCC cells with varied treatments were subcutaneously administered into the flanks of four to five-week-old male BALB/c nude mice (n=6 per group). Then, tumor volumes were determined using a Vernier caliper every week. At 5 weeks after cell injections, mice were sacrificed, tumors were harvested and their weights determined. The ethical committee of the Fourth Military Medical University for animal research approved the use of animals in this study. When tumors were 3 to 4mm in diameter, SR8278 at 0.5 mg/mice was administered in each tumor twice a week.

For the *in vivo* metastatic assay,  $5 \times 10^6$  HCC cells with varied treatments were intravenously administered into four to five-week-old male BALB/c nude mice via their tail veins (n=6 per group). Mice were sacrificed at two months after cell administration and their lungs collected for H&E staining. Metastatic tumor nodules in lungs were counted. SR8278 at dose of 0.5 mg/mice was administered into each mouse twice a week by intraperitoneal injection after operation.

### **Silencing and forced expressions of target genes**

To transiently silence BMAL1, small interference RNAs (siRNAs) targeting BMAL1 were transfected into HCC cells using the lipofectamine 2000 reagent (Invitrogen) as per the manufacturer's instructions. A pSilencer™ 3.1-H1 puro vector (Ambion) was used to construct the shRNA targeting BMAL1. To construct the BMAL1 over-expression vector, the BMAL1 coding sequence was amplified and cloned into a pcDNA™3.1(C) vector (Invitrogen).

### **Luciferase assay**

Luciferase assays were performed as previously described[1]. The HCC cells were co-transfected with 4 µg of GPAM promoter constructs and Renilla luciferase expressing control vector and grown for 48 h. Cells were lysed using the ice-cold lysis buffer after which luciferase enzyme activities were assessed by Dual Luciferase Reporter Assay (Promega, E1910), as instructed by the manufacturer. A Luminoscan Ascent Microplate Luminometer (Thermo Scientific) was used to determine the relative light units. Luciferase activities were standardized to renilla luciferase enzyme activities.

### **Chromatin immunoprecipitation (ChIP)-PCR assay**

The ChIP assay was performed using a ChIP assay kit (Cell Signaling, #9005), as per the manufacturers' protocol. The HCC cells were fixed in 1% formaldehyde and disrupted in the lysis buffer. Subsequently, samples were sonicated to degrade the nuclear membranes and the supernatants collected. Then, immune-precipitations of chromatin by an anti-BMAL1 antibody (1:100) or equivalent quantities of normal rabbit IgG were performed. DNA was isolated and PCR amplified using primer pairs within the modulatory site of GPAM, sequences of which are shown in **Supplementary Table 1**.

### **Co-immunoprecipitation (Co-IP) assay**

For co-IP assays, HCC cells were lysed in ice-cold lysis buffer and incubated overnight at 4°C with 25 µl protein A beads (Santa Cruz) enriched with anti-BMAL1 (1:500) and anti-GPAM (1:300) antibodies. After rinsing 3 times using cold washing buffer, immunoprecipitated samples were eluted by heating in a loading buffer at 100 °C for 5 mins, followed by immunoblotting (WB) for analysis.

### **Statistical analysis**

Data are shown as mean  $\pm$  SEM. The SPSS software (17.0 version, Chicago, IL) was used for analyses, with  $p < 0.05$  as the threshold for significance (\*). Overall and recurrence-free survival curves were computed using the Kaplan-Meier approach. Two-tailed student's t-test and one-way ANOVA followed by Tukey's post-hoc test were used for comparisons of means between and among groups, respectively. Relationships between measured variables were determined by Spearman rank

correlation analysis.

## Supplemental figures

**Figure S1:** Western blot analysis for BMAL1 expressions in 30 paired HCC and adjacent non-tumor tissues.

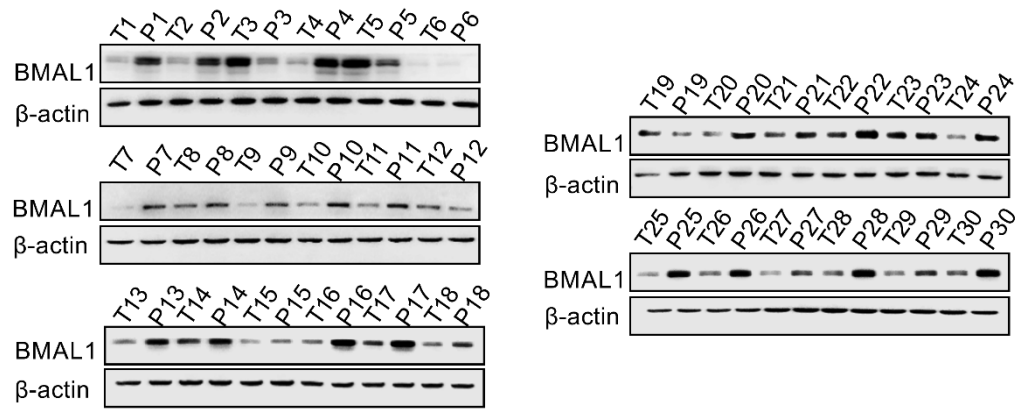


**Figure S2:** (A and B) Knockdown of BMAL1 in SNU-368 and SNU-739 cells was confirmed by qRT-PCR (A) and Western blot (B) analysis. (C) EdU incorporation assay for SNU-368 and SNU-739 cells with BMAL1 knocked-down (Scale bar, 50  $\mu\text{m}$ ). (D and E) Cell cycle distribution and apoptosis of treated SNU-368 and SNU-739 cells was evaluated by flow cytometry. (F and G) Western blot analysis for key regulators involved in regulation of cell cycle distributions and apoptosis of SNU-368 and SNU-739 cells with BMAL1 knocked-down. (H) Western blot analysis for expressions of EMT markers in treated SNU-368 and SNU-739 cells. (I) IHC staining of Ki-67 in tumor tissues from subcutaneous xenografts. Scale bar, 100  $\mu\text{m}$ . (J) TUNEL assay for tumor tissues from subcutaneous xenografts. Scale bar, 100  $\mu\text{m}$ .

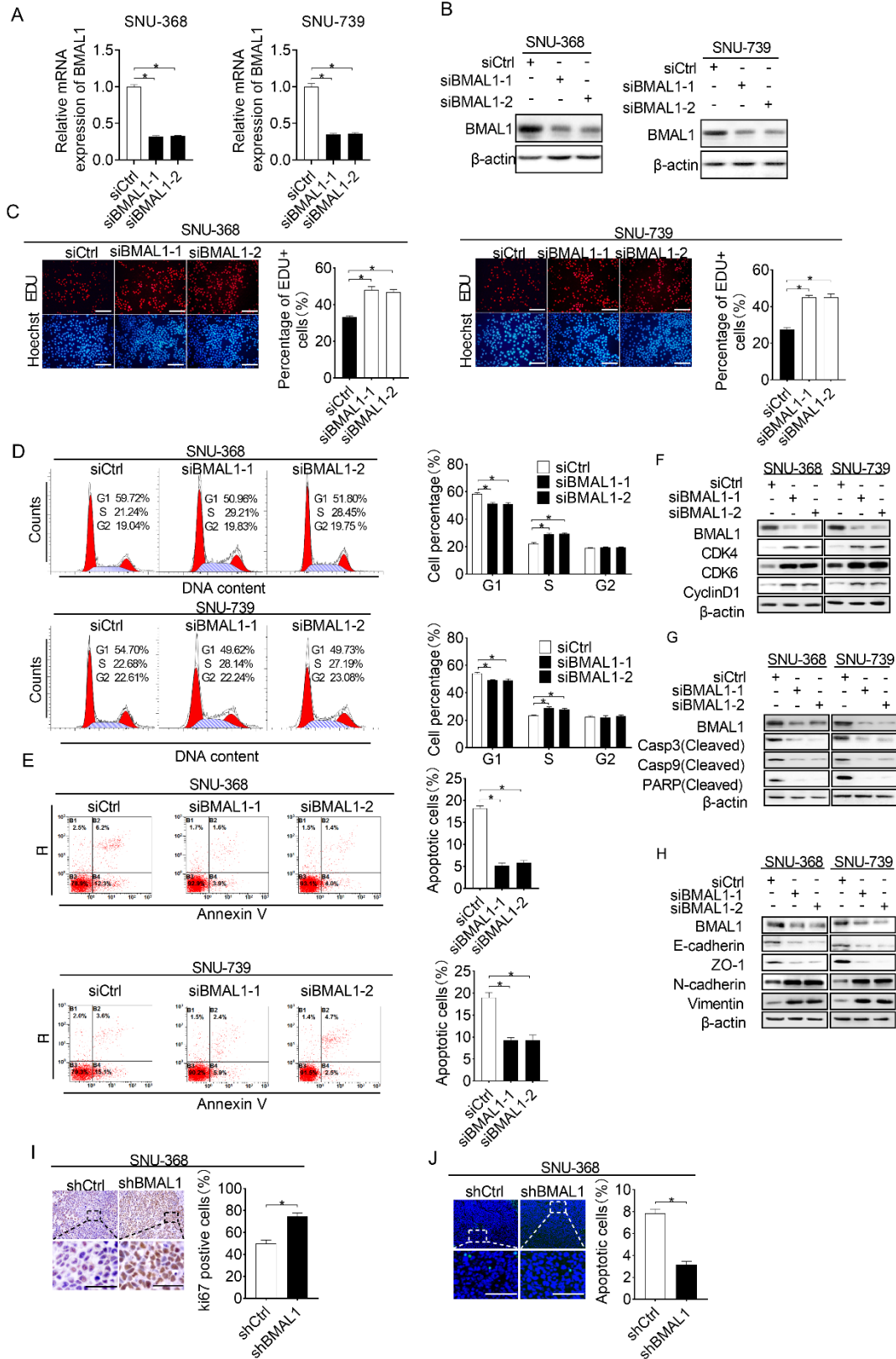


**Figure S3:** (A and B) Overexpressions of BMAL1 in MHCC97H and Hep3B cells were confirmed by qRT-PCR (A) and Western blot (B) analyses. (C) EdU incorporation assay for MHCC97H and Hep3B cells with BMAL1 overexpressed (Scale bar, 50  $\mu$ m). (D and E) Cell cycle distributions and apoptosis of MHCC97H and Hep3B cells with BMAL1 overexpressed were evaluated by flow cytometry. (F and G) Western blot analysis for key regulators of cell cycle distributions and apoptosis of MHCC97H and Hep3B cells with BMAL1 overexpressed. (H) Western blot analysis for expressions of EMT markers in MHCC97H and Hep3B cells with BMAL1 overexpressed. (I and J) Ki-67 IHC staining and TUNEL assays of tumor tissues from subcutaneous xenografts (Scale bar, 100  $\mu$ m).

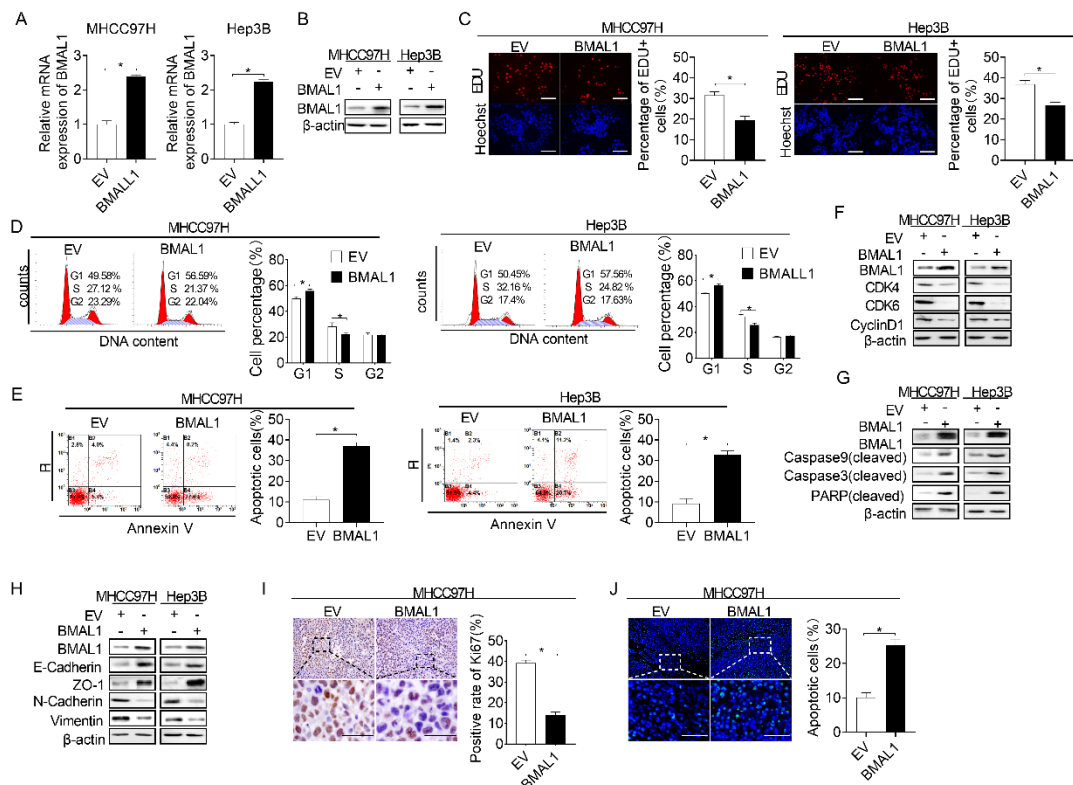


**Figure S4:** (A) IHC-staining for GPAM in 36-unpaired primary and metastatic HCC tissues. (B) Correlations between protein expression levels of BMAL1 and GPAM in 36-unpaired primary and metastatic HCC tissues. \* $p < 0.05$ . Scale bar: 100  $\mu\text{m}$ . (C) Expressions of GPAM were assessed by qRT-PCR (left) and western blot (right) assays ( $n=217$ ). (D) Correlations between protein expressions of BMAL1 and GPAM in HCC and normal hepatic cell lines. (E) Prognostic value of GPAM was determined by IHC staining ( $n=217$ ).

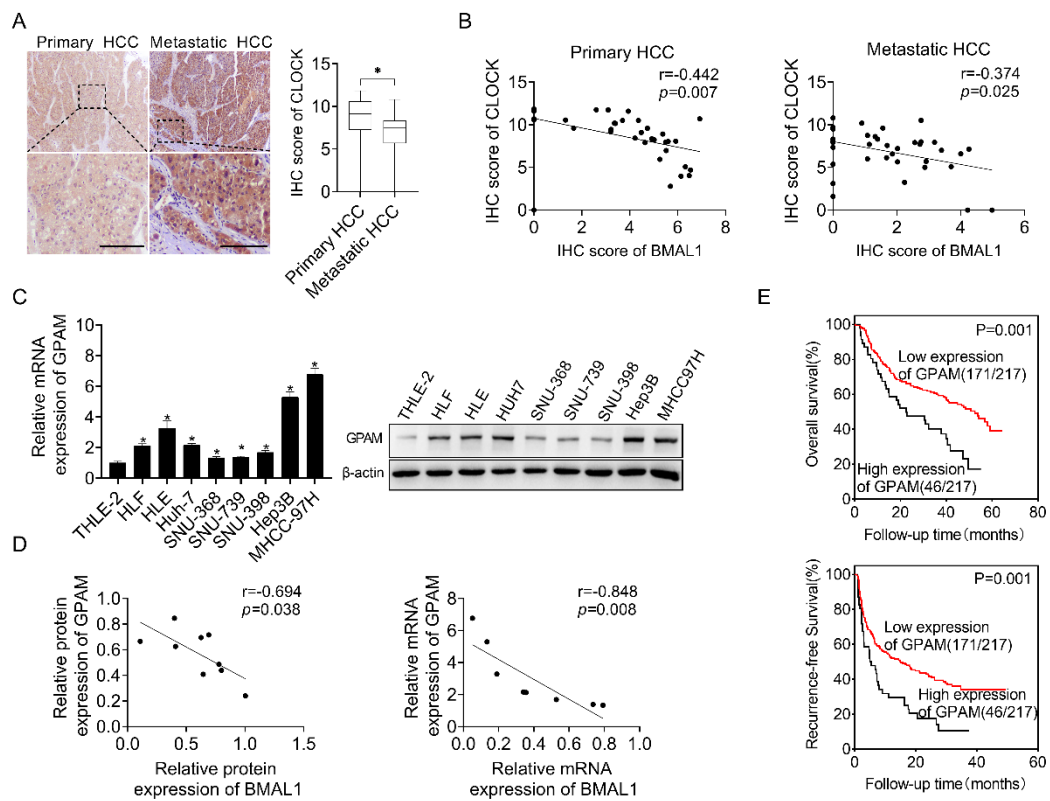


**Figure S5:** Correlations between BMAL1 expressions and levels of LPA, PA, DAG and TAG in tumor tissues from 30 HCC patients.

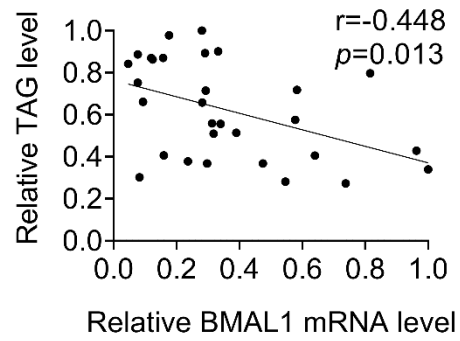
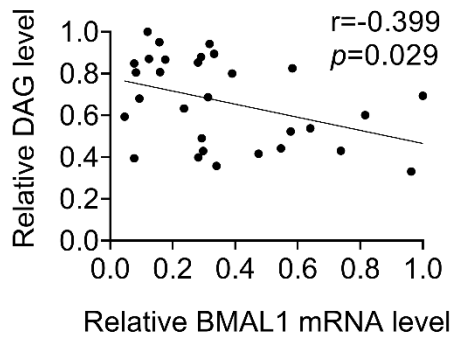
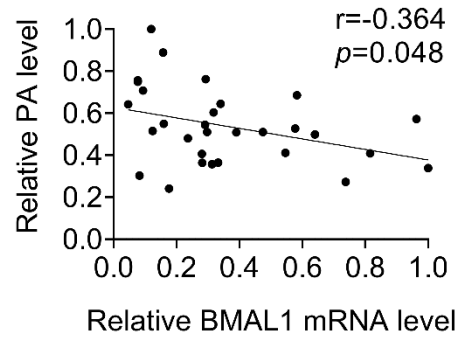
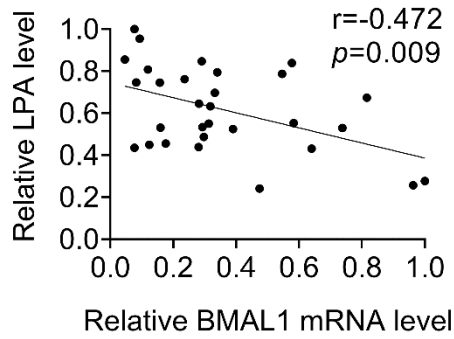


**Figure S6: BMAL1 is a target gene for miR-494-3p.** (A) Predicted binding sequence for miR-494-3p within the BMAL1 3'UTR. Seed sequences are highlighted. (B) Luciferase reporter assay for SNU-368 cells co-transfected with wild-type or mutant miR-494-3p and anti-miR-494-3p. (C) Luciferase reporter assay for MHCC97H cells co-transfected wild-type or mutant miR-494-3p and miR-494-3p mimics. NS: no significant difference.

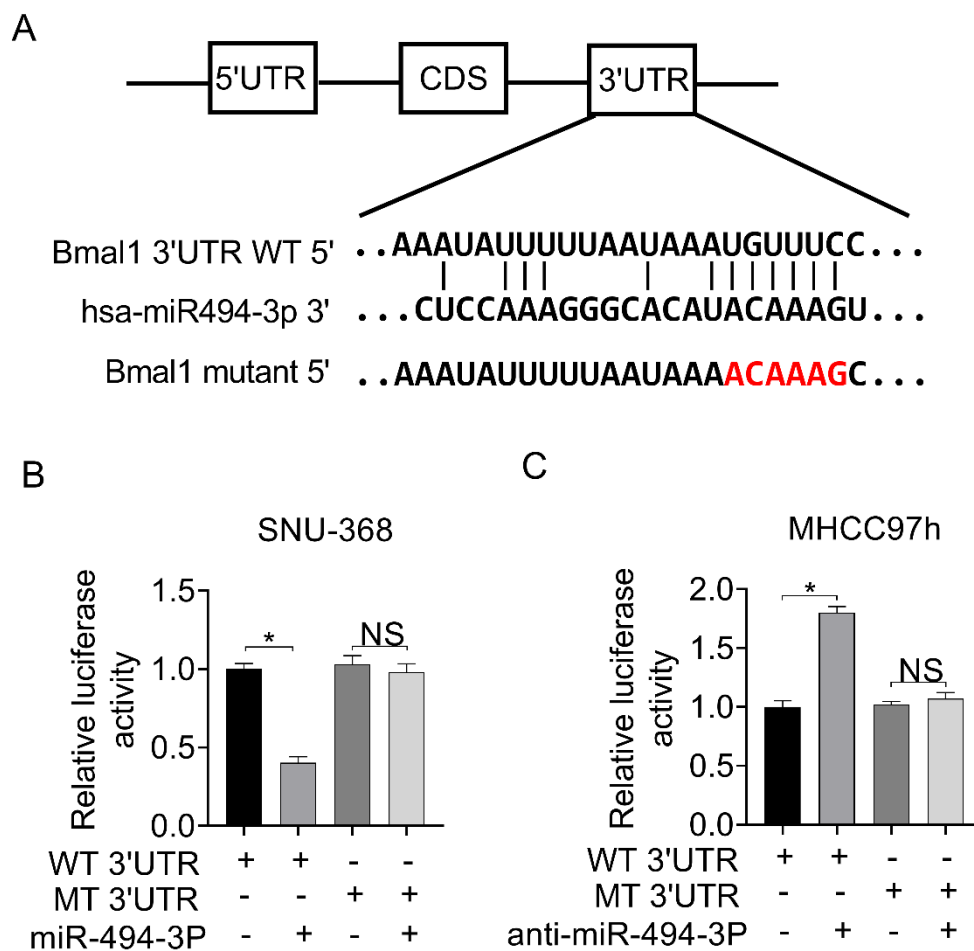
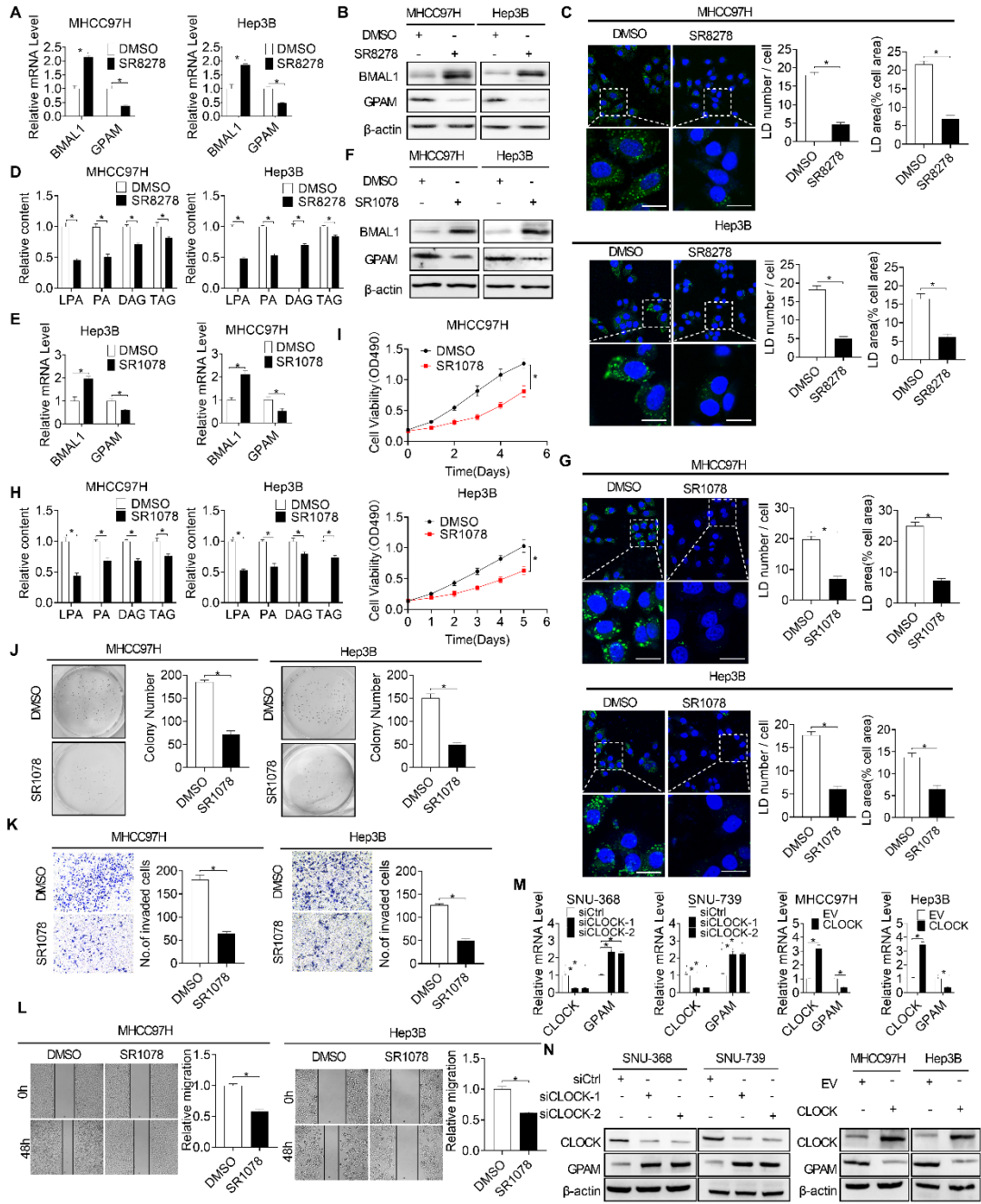


**Figure S7:** (A and B) qRT-PCR and western blot analysis for expressions of BMAL1 and GPAM in MHCC97H and Hep3B cells treated with the REV-ERB $\alpha$  antagonist, SR8278. (C) Levels of neutral lipids in MHCC97H and Hep3B cells treated with the REV-ERB $\alpha$  antagonist, SR8278, were detected by fluorescence BODIPY 493/503 dye staining. Scale bars, 50  $\mu$ m. Average number of LDs per cell and percentage of cellular area occupied by LDs were quantified. (D) Levels of G3P, PA, DAG, TAG and LPA in MHCC97H and Hep3B cells treated with SR8278 were detected by ELISA. (E and F) qRT-PCR and western blot analysis for expressions of BMAL1 and GPAM in MHCC97H and Hep3B cells treated with a ROR agonist, SR1078, at a concentration of 10  $\mu$ M for 24 h. (G) Levels of neutral lipids in MHCC97H and Hep3B cells treated with SR1078 were determined by fluorescence BODIPY 493/503 dye staining. Scale bars, 50  $\mu$ m. Average number of LDs per cell and percentage of cellular area occupied by LDs were quantified. (H) Levels of G3P, PA, DAG, TAG and LPA in MHCC97H and Hep3B cells treated with SR1078 were detected by ELISA. (I and J) MTS and colony formation assays were conducted for MHCC97H and Hep3B cells exposed to SR1078. (K and L) Scratch-wound-healing and matrigel invasion assays for MHCC97H and Hep3B cells treated with SR1078.



## Supplementary Tables

**Table S1: Sequences of primers, siRNAs and miRNAs used in this study.**

<b>1. Primers used in q-PCR analysis</b>		
<i>BMAL1</i>	forward primer	GGATGTGACCGAGGGAAGAT
	reverse primer	CGTCGTGCTCCAGAACATAAT
<i>GPAM</i>	forward primer	GATGTAAGCACACAAGTGAGGA
	reverse primer	TCCGACTCATTAGGCTTTCTTTC
<i>MGLL</i>	forward primer	GCTCTCGAGGCCGCCATGCCAGAGGAAAGTTCC
	reverse primer	AGCTGAATTCTCAGGGTGGGGACGCAGTTCCTG
<i>DGAT2</i>	forward primer	ATTGCTGGCTCATCGCTGT
	reverse primer	GGGAAAGTAGTCTCGAAAGTAGC
<i>PPAP2B</i>	forward primer	TGAGAGCATCAAGTACCCACT
	reverse primer	ACGTAGGGGTTCTGAATCGTC
miR-494-3p	forward primer	ACACTCCAGCTGGG TGAAACATACACGGGA
	reverse primer	CTCAACTGGTGTCTCGTGGAGTCGGCAATTCAGTTG
U6	forward primer	CTCGCTTCGGCAGCACA
	reverse primer	AACGCTTCACGAATTTGCGT
<i>GAPDH</i>	forward primer	GGAGCGAGATCCCTCCAAAAT
	reverse primer	GGCTGTTGTCATACTTCTCATGG
<i>CLOCK</i>	forward primer	GCTCGAGGGTGGCTGGGAGTTTTGATTG
	reverse primer	GCTCTAGACACGTTTAGAAGGCATGTGAGTTAC
<b>2. Primers for <i>GPAM</i> promoter construct</b>		
(-2076/+86) <i>GPAM</i>	forward primer:	CGGGATCCCGCCTCCCGTCAGGTTTT TTACTG
(-929/+86) <i>GPAM</i>	forward primer:	CGGGATCCCGCTCAAGGCAATCATAG GGC
(-428/+86) <i>GPAM</i>	forward primer:	CGGGATCCCGCGCACTCAGCCACTTT GGTA
(-102/+86) <i>GPAM</i>	forward primer:	CGGGATCCCGCATCCGCTCACGCTCC C
	reverse primer:	CCATCGATGGCTGGCAGTTCGCACCC TA
<b>3. Primers for <i>GPAM</i> promoter site-directed mutagenesis</b>		

(-428/+86) GPAM mutation forward	GTGAGCGCCTGGACGGACGGTTACCCTGC CTA
(-428/+86) GPAM mutation reverse	TAGGCAGGGTAACCGTCCGTCCAGGCGCTC AC

#### 4. Primers used for *BMAL1* site-directed mutagenesis

BMAL1 mutation forward	GTATTATAGAACAAGGCTTCTCTTTATTA AATATTAACTGTCTAGT
BMAL1 mutation reverse	ACTAGACAGTTAAATATTTTAATAAAGAG AAGCCTTGTTCTATAATAC

#### 5. Primers used for ChIP in the *GPAM* promoter

<i>GPAM</i>	forward primer	GCAACAGATGAATCCCTA
	reverse primer	TGAATTCCTGAGAACCC

#### 6. siRNAs

Gene	sense	anti-sense
siBMAL1-1	GCUCUUUCUUCUGUAGA AUTT	AUUCUACAGAAGAAAGAGCTT
siBMAL1-2	GCCUUCAGUAAAGGUUG AA	UUCAACCUUUACUGAAGGC
siGPAM	CAAUCAAAAGCCGUUAA CA	UGUUAACGGCUUUUGAUUG
siCLOCK-1	ACGAGA ACTTGGCATT GAA	UUCA AUGCCAAGUUCUCGU
siCLOCK-2	CAAGATTCTGGGTCAG ATA	UAUCUGACCCAGAAUCUUG
siControl	UUCUCCGAACGUGUCAC GUTT	ACGUGACACGUUCGGAGAATT

#### 7. miR-494-3p and anti-mi-494-3p

Gene	sense	anti-sense
miR-494-3p mimics	UGAAACAUCACGGGAAA CCUC	GGUUUCCCGUGUAUGUUUCAUU
miR-494-3p inhibitor	GAGGUUUCCCGUGUAUGU UUCA	
miR-27b-3p mimics	UUCACAGUGGCUAAGUUC UGC	AGAACUUAGCCACUGUGAAUU
miR-141-3p mimics	UAACACUGUCUGGUAAG AUGG	ACAUAGGAAUAAAAAGCCAUAU U
miR-141-3p mimics	UAACACUGUCUGGUAAG AUGG	AUCUUUACCAGACAGUGUUAUU
miR-155-5p mimics	UUAAUGC UAAUCGUGAUA GGGGUU	CCCCUAUCACGAUUAGCAUUAUU U

**Table S2:** Primary antibodies used in this study.

<b>Antibody</b>	<b>Company (Cat. No.)</b>	<b>Working dilutions</b>
BMAL1	NOVUS (NB100-2288)	WB: 1/1000; IHC:1/1000; IF: 1/200; IP:1/100; ChIP:1/100;
GPAM	SANTA (sc-398135)	WB: 1/1000; IHC:1/200
EZH2	CST (3147S)	IF: 1/200
EZH2	Abcam (191250)	IP:1/50
cleaved caspase-9	Abcam(ab2324)	WB: 1/1000
cleaved caspase-3	Abcam(ab2302)	WB: 1/500
cleaved PARP	Abcam(ab194217)	WB: 1/1000
CDK4	Proteintech(11026-1-AP)	WB: 1/500
CDK6	Proteintech (14052-1-AP)	WB: 1/1000
Cyclin D1	Proteintech(60186-1-AP)	WB: 1/1000
E-cadherin	Proteintech(20874-1-AP)	WB: 1/500
ZO-1	Proteintech(21773-1-AP)	WB: 1/1000
N-cadherin	Cell Signaling (13116)	WB: 1/1000
Vimentin	Proteintech(10366-1-AP)	WB: 1/1000
Ki-67	Abcam(ab15580)	IHC:1/250
CLOCK	Proteintech(13463-1-AP)	WB:1/500
$\beta$ -actin	Beijing TDY(TDY051F)	WB: 1/3000

**Table S3: Correlations between expressions of BMAL1 and clinic-pathologic features of 217 HCC patients.**

Variables	No. of cases (%)	BMAL1 expression		<i>P</i> value
		Low	High	
All	217 (100%)	118	99	
Age				
<55	53	25	28	0.226
>=55	164	93	71	
Gender				
Female	35	19	16	0.991
Male	182	99	83	
HBV				
Negative	15	7	8	0.557
Positive	202	111	91	
AFP (ug/ml)				
<200	159	86	73	0.887
>=200	58	32	26	
Maximum diameter of lesion				
<5	92	42	50	<b>0.027</b>
>=5	125	76	49	
PVTT				
No	191	97	94	<b>0.004</b>
Yes	26	21	5	
TNM stage				
I+ II	32	22	10	0.078
III+ IV	185	96	89	
Treatment				
Hepatectomy	90	48	42	0.795
Hepatectomy+		70	57	
TACE	127			

**Abbreviations:** AFP, alpha-fetoprotein; PVTT, portal vein tumor thrombosis; TNM, tumor-nodes-metastases; TACE, transcatheter arterial chemoembolization.

**Table S4: Univariate analysis of potential predictors for OS in 217 HCC patients.**

Variables	No. of cases (%)	Median of OS time(months)	<i>P</i> value
Age			
<55	53	33.1	0.829
>=55	164	37.8	
Gender			
Female	35	33.5	0.105
Male	182	39.5	
HBV			
Negative	15	41.3	0.495
Positive	202	34.7	
AFP (ug/ml)			
<200	159	40.3	<b>0.001</b>
>=200	58	11.6	
Maximum diameter of lesion			
<5	92	40.5	<b>0.011</b>
>=5	125	30.4	
PVTT			
No	191	39.9	<b>0.001</b>
Yes	26	11.6	
TNM stage			
I+ II	32	46.6	<b>0.003</b>
III+ IV	185	31.8	
Treatment			
Hepatectomy	90	34.9	0.375
Hepatectomy+ TACE	127	37.8	

**Table S5: Univariate analysis of potential predictors for RFS in 217 HCC patients.**

Variables	No. of cases (%)	Median of RFS time (months)	<i>P</i> value
Age			
<55	53	8.3	0.413
>=55	164	11.0	
Gender			
Female	35	14.8	0.410
Male	182	8.5	
HBV			
Negative	15	9.0	0.631
Positive	202	18.3	
AFP (ug/ml)			
<200	159	17.4	<b>0.001</b>
>=200	58	2.6	
Maximum diameter of lesion			
<5	92	17.7	<b>0.001</b>
>=5	125	6.7	
PVTT			
No	191	15.0	<b>0.001</b>
Yes	26	2.5	
TNM stage			
I+ II	32	24.6	0.001
III+ IV	185	7.3	
Treatment			
Hepatectomy	90	9.3	0.239
Hepatectomy+		11.0	
TACE	127		

**Table S6. Multivariate analysis of potential predictors for OS in 217 HCC patients (BMAL1) .**

Variables	HR	95%CI	<i>P</i> value
AFP	2.453	1.676-3.590	0.001
Maximum diameter of lesion	1.785	1.201-2.653	0.004
PVTT	3.678	2.208-6.128	0.001
TNM stage	1.877	1.007-3.499	0.047
BMAL1	0.598	0.403-0.889	0.011

**Table S7. Multivariate analysis of potential predictors for RFS in 217 HCC patients (BMAL1).**

Variables	HR	95%CI	<i>P</i> value
AFP	2.404	1.700-3.401	0.001
Maximum diameter of lesion	1.849	1.288-2.654	0.001
PVTT	2.930	1.788-4.802	0.001
TNM stage	2.610	1.424-4.784	0.002
BMAL1	0.511	0.358-0.731	0.001

**Table S8. Multivariate analysis of potential predictors for OS in 217 HCC patients (GPAM) .**

Variables	HR	95%CI	<i>P</i> value
AFP	2.649	1.811-3.876	0.001
Maximum diameter of lesion	2.023	1.364-3.001	0.001
PVTT	5.119	3.112-8.420	0.001
GPAM	2.257	1.494-3.410	0.001

**Table S9. Multivariate analysis of potential predictors for RFS in 217 HCC patients (GPAM).**

Variables	HR	95%CI	<i>P</i> value
AFP	2.437	1.720-3.453	0.001
Maximum diameter of lesion	2.097	1.469-2.996	0.001
PVTT	4.079	2.508-6.636	0.001
TNM stage	1.988	1.088-3.633	0.026
GPAM	2.057	1.412-2.997	0.001

## Reference

1. Yuan P, Li J, Zhou F, Huang Q, Zhang J, Guo X, et al. NPAS2 promotes cell survival of hepatocellular carcinoma by transactivating CDC25A. *Cell death & disease*. 2017; 8: e2704.
2. Zhao J, Zhang X, Gao T, Wang S, Hou Y, Yuan P, et al. SIK2 enhances synthesis of fatty acid and cholesterol in ovarian cancer cells and tumor growth through PI3K/Akt signaling pathway. *Cell Death Dis*. 2020; 11: 25.
3. Zhao J, Hou Y, Yin C, Hu J, Gao T, Huang X, et al. Upregulation of histamine receptor H1 promotes tumor progression and contributes to poor prognosis in hepatocellular carcinoma. *Oncogene*. 2020; 39: 1724-38.
4. Zhang H, Fan J, Wang J, Dou B, Zhou F, Cao J, et al. Fluorescence discrimination of cancer from inflammation by molecular response to COX-2 enzymes. *J Am Chem Soc*. 2013; 135: 17469-75.
5. Zhang H, Fan J, Wang K, Li J, Wang C, Nie Y, et al. Highly sensitive naphthalene-based two-photon fluorescent probe for in situ real-time bioimaging of ultratrace cyclooxygenase-2 in living biosystems. *Anal Chem*. 2014; 86: 9131-8.